Enhancing Power Efficiency in MIMO DFT-s-OFDM: A Relative Study of π/2-BPSK with Tone Reservation

Abhinaba Dey
Systems R&D,
Lekha Wireless Solutions
Bengaluru, India
abhinabadey@ieee.org

Sreenath Ramanath
Systems R&D,
Lekha Wireless Solutions
Bengaluru, India
ramanath.sreenath@gmail.com

***Abstract*—Peak-to-average power ratio (PAPR) remains a crucial restriction in multicarrier systems, even in single-carrier precoding methods such as discrete Fourier transform-spread orthogonal frequency domain multiplexing (DFT-s-OFDM), especially under multi-antenna transmission. This article introduces a comparative analysis of PAPR and bit error rate (BER) performance for QPSK DFT-s-OFDM, π/2-BPSK DFT-s-OFDM, and π/2-BPSK DFT-s-OFDM with tone reservation (TR) in a multiple-input-multiple-output (MIMO) framework. The π/2-BPSK modulation naturally provides better signal envelope characteristics, while TR is used to further minimize PAPR by using reserved subcarriers without altering the data-bearing tones. To guarantee equitable comparison across all schemes, a single simulation framework with uniform channel modelling and receiver processing is created. The findings show that, in comparison to QPSK DFT-s-OFDM, π/2-BPSK DFT-s-OFDM yields a good PAPR reduction; however, incorporation of TR offers a large additional PAPR decrease. These results offer practical design guidance for next-generation wireless systems' power-efficient uplink transmission.**

***Index Terms*—DFT-s-OFDM, Peak-to-average power ratio (PAPR) reduction, Tone reservation, Uplink transmission, Precoding techniques, π/2-BPSK, MIMO framework**

I. Introduction

For contemporary wireless communication systems, energy-efficient waveform design is essential, especially in uplink transmissions when user equipment is subject to stringent power limitations. The high peak-to-average power ratio (PAPR) in multicarrier systems presents a significant difficulty since it requires the power amplifier (PA) to operate with large back-off, which lowers coverage and power efficiency [1].

Discrete Fourier transform spread orthogonal frequency division multiplexing (DFT-s-OFDM), sometimes referred to as single-carrier frequency division multiple access (SC-FDMA), has been extensively used in LTE and 5G New Radio (NR) uplink to solve the issue at hand [2]. Compared to traditional cyclic prefix OFDM (CP-OFDM), DFT-s-OFDM has an intrinsically lower PAPR because of its single-carrier structure, which improves PA efficiency. Nevertheless, DFT-s-OFDM still experiences residual envelope fluctuations in spite of this benefit, particularly when bandwidth, subcarrier allocation, and multi-antenna transmission increase [3], [4], [5].

Simultaneously, in order to improve spectrum efficiency and link dependability, multiple-input multiple-output (MIMO) techniques have become an essential component of contemporary wireless systems. Independent data streams are sent from several antennas during MIMO uplink transmission, which can exacerbate instantaneous power fluctuations across transmit branches. This increases the importance of PAPR reduction in realistic MIMO DFT-s-OFDM systems [6].

The literature has suggested a number of PAPR reduction strategies, which can be broadly divided into distortion-based and distortionless approaches. Although distortion-based methods like clipping and companding [7] are easy to use, they cause spectrum regrowth and BER degradation by introducing in-band distortion and out-of-band emissions. However, distortionless methods such as tone reservation (TR), selective mapping (SLM) [8], and precoding-based approaches [9] avoid these problems at the expense of higher complexity or a decrease in spectral efficiency.

$\pi/2$-BPSK has drawn a lot of interest among precoding-based methods because of its advantageous envelope properties, which are attained by deterministic phase rotation. Because of its increased power efficiency, it has been implemented in 5G NR uplink control channels [10]. By assigning a fraction of subcarriers to produce peak-canceling signals, tone reservation (TR) independently lowers PAPR without causing distortion to data-bearing tones or necessitating side information at the receiver [11].

The relative performance of $\pi/2$-BPSK and TR inside a DFT-s-OFDM framework, especially under MIMO transmission, is not clearly characterised, despite the fact that both individually provide PAPR reduction benefits. Furthermore, a comprehensive framework is needed to carefully assess any possible trade-off between bit error rate (BER) performance and PAPR reduction in such systems. Inspired by these factors, this work compares three DFT-s-OFDM schemes in a MIMO setting, which are, QPSK DFT-s-OFDM, $\pi/2$-BPSK DFT-s-

OFDM, and $\pi/2$-BPSK DFT-s-OFDM with tone reservation. To assess PAPR (using the complementary cumulative distribution function (CCDF)) and BER performance under the same channel conditions, a consistent simulation framework is created.

The novelty of this work does not lie in proposing a new PAPR reduction technique. Rather, its contribution is threefold:

- Development of a unified MIMO DFT-s-OFDM simulation framework enabling direct comparison of QPSK DFT-s-OFDM, $\pi/2$-BPSK DFT-s-OFDM, and $\pi/2$-BPSK with TR under identical assumptions.
- Quantitative evaluation of the trade-off among PAPR, BER, spectral efficiency, and computational complexity in multi-antenna uplink transmission.
- Practical design insights regarding the suitability of $\pi/2$-BPSK and TR for power-efficient 5G NR and future wireless uplink systems.

The findings shed light on whether these methods are appropriate for power-efficient uplink transmission in upcoming multi-antenna wireless systems.

II. System Model

A. MIMO DFT-s-OFDM Transmission

Consider a MIMO based DFT-s-OFDM system having N_t transmit and N_r receive antennas. Let M represents the number of data symbols per transmit antenna and N is the IDFT size, in which $N \geq M$. The set of data subcarriers is represented by $\mathcal{S}_D$, whereas $\mathcal{S}_R$ denotes the reserved subcarriers utilized for tone reservation, in a manner that $\mathcal{S}_D \cap \mathcal{S}_R = \emptyset$.

Considering each transmit antenna $t \in \{1, \ldots, N_t\}$, the complex symbols are mapped from input bit sequence forming

$$\mathbf{d}^{(t)} = [d_0^{(t)}, d_1^{(t)}, \ldots, d_{M-1}^{(t)}]^T. \tag{1}$$

DFT spreading is employed independently per antenna:

$$\mathbf{D}^{(t)} = \mathbf{F}_M \mathbf{d}^{(t)} \tag{2}$$

where $\mathbf{F}_M$ represents the normalized M-point DFT matrix.

The frequency-domain signal is built as

$$X^{(t)}[k] = \begin{cases} D^{(t)}[m], & k \in \mathcal{S}_D \\ 0, & \text{otherwise} \end{cases} \tag{3}$$

and the time-domain signal is acquired via IDFT:

$$\mathbf{x}^{(t)} = \mathbf{F}_N^H \mathbf{X}^{(t)}. \tag{4}$$

A cyclic prefix (CP) is appended prior to transmission.

B. MIMO Channel Model

The resultant signals get transmitted through a frequency-flat Rayleigh fading channel denoted by matrix $\mathbf{H} \in \mathbb{C}^{N_r \times N_t}$. The signal received at time index n is given by

$$\mathbf{y}[n] = \mathbf{H}\mathbf{x}[n] + \mathbf{w}[n] \tag{5}$$

in which $\mathbf{w}[n] \sim \mathcal{CN}(0, \sigma^2 \mathbf{I})$ is additive white Gaussian noise.

After removing the CP, FFT is employed to get the frequency-domain received signal:

$$\mathbf{Y}[k] = \mathbf{H}\mathbf{X}[k] + \mathbf{W}[k]. \tag{6}$$

C. Modulation Schemes

1) QPSK DFT-s-OFDM: In QPSK modulation, symbols are obtained from

$$d \in \left\{ \frac{1}{\sqrt{2}}(\pm 1 \pm j) \right\} \tag{7}$$

and are directly DFT-spreaded.

2) $\pi/2$-BPSK DFT-s-OFDM: For $\pi/2$-BPSK, binary symbols $a_n^{(t)} \in \{\pm 1\}$ get rotated as

$$s_n^{(t)} = a_n^{(t)} e^{j\frac{\pi}{2}n}. \tag{8}$$

The rotated symbols get DFT-spreaded prior to subcarrier mapping. This phase rotation mechanism enhances the temporal envelope features of the transmitted signal.

D. Tone Reservation (TR)

In TR, a portion of the subcarriers $\mathcal{S}_R$ is reserved to produce peak-canceling signals. The transmitted signal is defined as

$$\mathbf{X}^{(t)} = \mathbf{X}_D^{(t)} + \mathbf{X}_R^{(t)} \tag{9}$$

where $\mathbf{X}_R^{(t)}$ is non-zero only on $\mathcal{S}_R$.

An iterative clipping and projection mechanism is utilized. The time-domain signal is clipped as

$$\bar{x}[n] = \begin{cases} x[n], & |x[n]| \leq A \\ Ae^{j\angle x[n]}, & |x[n]| > A \end{cases} \tag{10}$$

The clipping noise is calculated as

$$\mathbf{e} = \bar{\mathbf{x}} - \mathbf{x} \tag{11}$$

and projected upon the reserved tones:

$$\mathbf{X}_R^{(t)} \leftarrow \mathcal{P}_{\mathcal{S}_R}(\mathbf{F}_N \mathbf{e}) \tag{12}$$

while keeping data tones unaltered.

E. Receiver Processing

Zero-forcing (ZF) equalization is employed per subcarrier:

$$\hat{\mathbf{X}}[k] = \mathbf{H}^{\dagger}\mathbf{Y}[k] \tag{13}$$

where $\mathbf{H}^{\dagger}$ represents the pseudo-inverse of $\mathbf{H}$.

The estimated data symbols are obtained and inverse DFT spreading is employed:

$$\hat{\mathbf{d}}^{(t)} = \mathbf{F}_M^H \hat{\mathbf{D}}^{(t)}. \tag{14}$$

For $\pi/2$-BPSK, de-rotation is applied prior to symbol detection.

F. PAPR and BER Metrics

The PAPR for the t-th transmit antenna is determined as

$$\text{PAPR}^{(t)} = \frac{\max_n |x^{(t)}[n]|^2}{\mathbb{E}[|x^{(t)}[n]|^2]}. \tag{15}$$

The complementary cumulative distribution function (CCDF) is utilized to differentiate PAPR:

$$\text{CCDF}(\gamma) = \Pr(\text{PAPR} > \gamma). \tag{16}$$

The bit error rate (BER) is calculated by analyzing transmitted and detected bits across all antennas over various E_b/N_0 values.

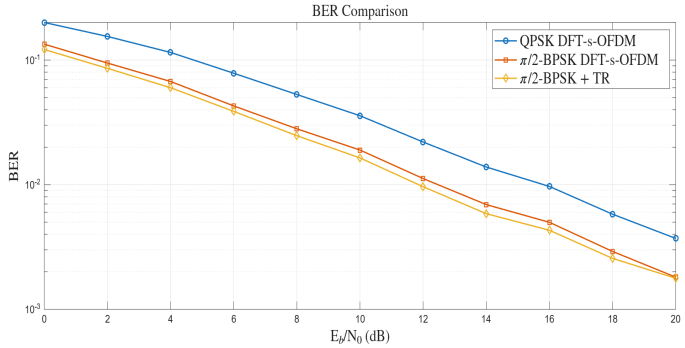

(a) BER (2×2 MIMO)

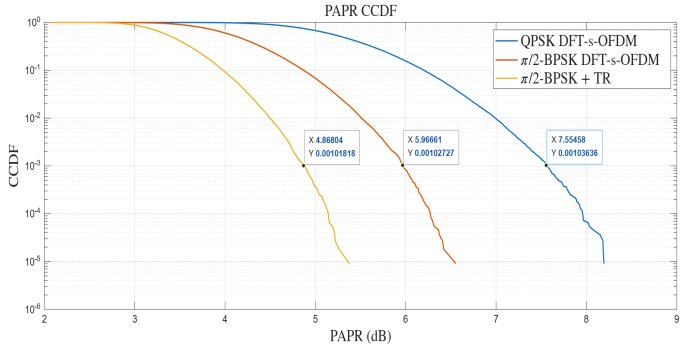

(b) PAPR CCDF (2×2 MIMO)

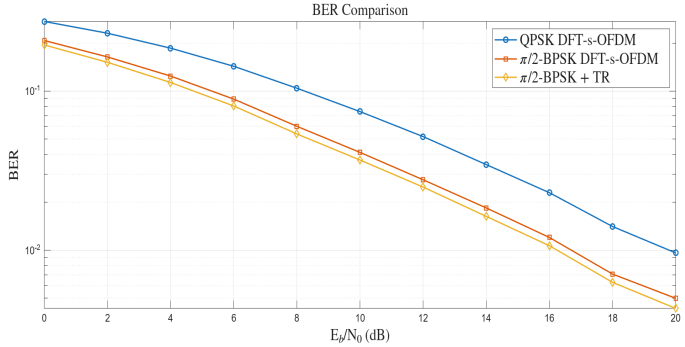

(c) BER (4×4 MIMO)

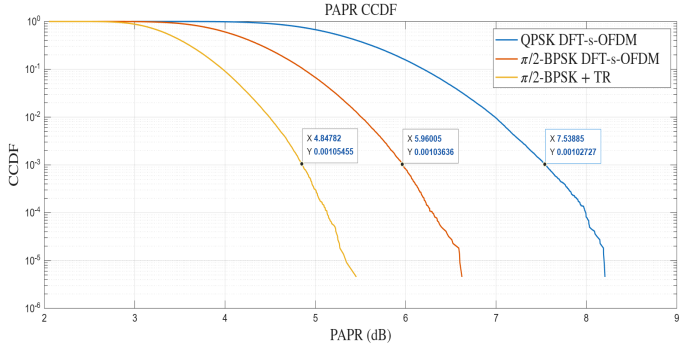

(d) PAPR CCDF (4×4 MIMO)

Fig. 1: Performance comparison of QPSK DFT-s-OFDM, $\pi/2$-BPSK DFT-s-OFDM, and $\pi/2$-BPSK with TR under 2×2 and 4×4 MIMO configurations.

III. Results and Discussion

A. Simulation Parameters

MATLAB-based link-level simulations are used to assess the performance of the MIMO DFT-s-OFDM systems under consideration. To guarantee fair comparison of QPSK DFT-s-OFDM, $\pi/2$-BPSK DFT-s-OFDM, and $\pi/2$-BPSK with tone reservation (TR), a single framework is used. In a frequency-flat Rayleigh fading channel, the system takes into account a 2×2 and 4×4 MIMO configuration. Important factors are maintained constant in all scenarios, including subcarrier allocation, modulation techniques, TR design, and detection strategy. Table I provides a summary of the specific simulation parameters.

TABLE I: Simulation Parameters for MIMO DFT-s-OFDM Schemes

Parameter	**Value**
MIMO configuration	2×2, 4×4
IDFT/FFT size (N)	128
Number of data subcarriers (M)	64
Subcarrier mapping	Localized
Cyclic prefix length	16
Number of OFDM symbols	5000
Modulation schemes	QPSK, $\pi/2$-BPSK
DFT spreading	Applied per transmit antenna
Tone reservation ratio	15% of data subcarriers
Number of reserved tones	≈ 10
TR iterations	5
Clipping threshold (A)	$1.3 \times \text{rms}(x[n])$
Channel model	Rayleigh flat fading
Noise model	AWGN
Equalization	Zero-forcing (ZF)
E_b/N_0 range	0 – 20 dB
PAPR evaluation	CCDF

B. Simulation Results and Discussion

Fig. 1 gives the BER and PAPR performance of the considered techniques under 2×2 and 4×4 MIMO configurations.

1) BER Performance Analysis: QPSK DFT-s-OFDM shows the highest BER over the whole E_b/N_0 range, according to Fig. 1(a) and (c). On the other hand, $\pi/2$-BPSK DFT-s-OFDM often performs better than QPSK, offering a discernible improvement in BER. The continuous envelope and enhanced phase continuity of $\pi/2$-BPSK, which improves robustness against noise and channel impairments, contribute to this improvement.

Tone reserve (TR) exhibits slight variance because of implementation and clipping threshold, but it does not deteriorate BER. Tone reservation (TR) primarily targets PAPR reduction and is not expected to directly improve BER under ideal linear transmission conditions. The simulation results indicate that TR maintains BER performance comparable to that of $\pi/2$-BPSK DFT-s-OFDM while providing substantial PAPR reduction. Minor BER variations observed at certain SNR values are attributed to finite simulation effects rather than

TABLE II: PAPR Comparison at CCDF = 10^{-3}

Scheme	2×2 **MIMO (dB)**	4×4 **MIMO (dB)**
QPSK DFT-s-OFDM	7.59	7.51
$\pi/2$-BPSK DFT-s-OFDM	5.93	5.94
$\pi/2$-BPSK + TR	4.83	4.87

an inherent BER advantage of TR. At moderate-to-high SNR values, the improvement is more noticeable.

When comparing 2×2 and 4×4 MIMO systems, it is found that higher-order MIMO results in a modest decline in overall BER performance. Enhanced spatial interference and noise amplification in zero-forcing (ZF) detection are likely to cause this. Nonetheless, both configurations exhibit the same relative performance trajectory among the three methods.

2) PAPR Performance Analysis: The PAPR CCDF plots in Fig. 1(b) and (d) distinctly substantiate the benefit of $\pi/2$-BPSK and TR.

At a CCDF of 10^{-3}:

- QPSK DFT-s-OFDM demonstrates the highest PAPR (around 7.5–7.6 dB),
- $\pi/2$-BPSK minimizes PAPR by approximately 1.5–1.6 dB,
- $\pi/2$-BPSK with TR attains the lowest PAPR (around 4.8–5.0 dB), providing a total increase of nearly 2.5–3 dB over QPSK.

There are two reasons for this improvement:
(i) the signal envelope is smoothed by the intrinsic phase rotation in $\pi/2$-BPSK, and
(ii) the TR mechanism uses reserved subcarriers to actively suppress peaks.

3) Impact of MIMO Order on PAPR: It is clear from comparing Fig. 1(b) and 1(d) that the PAPR distributions for 2×2 and 4×4 MIMO are almost the same. This is due to the fact that PAPR is calculated for each transmit antenna and that the statistical distribution of every transmit signal is not substantially changed by spatial multiplexing.

4) Overall Trade-off Analysis: The results detail a clear trade-off:

- QPSK DFT-s-OFDM produces baseline performance but sustains a higher PAPR.
- $\pi/2$-BPSK improves both PAPR and BER without extra complexity.
- $\pi/2$-BPSK with TR attains the best PAPR performance with a little betterment in BER, at the cost of decreased spectral efficiency due to reserved tones.

For uplink MIMO communications in next-generation wireless systems, the combination of $\pi/2$-BPSK with TR offers the most power-efficient approach overall.

The PAPR values at a CCDF of 10^{-3} are summarised in Table II. When compared to QPSK DFT-s-OFDM, $\pi/2$-BPSK is found to produce a reduction of roughly 1.6 dB, and the addition of TR results in an extra 1 dB gain. In comparison to QPSK, $\pi/2$-BPSK with TR yields an overall PAPR decrease of around 2.7 dB. Additionally, the PAPR values are almost the same for both 2×2 and 4×4 MIMO systems, indicating that PAPR is essentially independent of the number of transmit antennas when analysed per antenna.

C. Spectral Efficiency Impact of Tone Reservation

The use of tone reservation reduces the number of subcarriers available for data transmission. If M denotes the total number of allocated subcarriers and N_R denotes the number of reserved tones, the effective spectral efficiency is

$$\eta = \eta_0 \left(1 - \frac{N_R}{M}\right) \tag{17}$$

where η_0 represents the spectral efficiency without tone reservation.

For the considered configuration, approximately 10 out of 64 allocated subcarriers are reserved for TR. Consequently, the spectral efficiency reduction is

$$\frac{10}{64} \times 100 \approx 15.6\%. \tag{18}$$

This reduction represents the principal trade-off associated with the additional PAPR reduction achieved by TR.

TABLE III: Spectral Efficiency Comparison

Scheme	Reserved Tones	Efficiency Loss
QPSK DFT-s-OFDM	0	0%
$\pi/2$-BPSK DFT-s-OFDM	0	0%
$\pi/2$-BPSK + TR	10/64	15.6%

D. Complexity Analysis

The computational complexity of the methods under consideration is compared in Table IV. The baseline is QPSK DFT-s-OFDM, which uses normal DFT and IDFT procedures. Because of its straightforward phase rotation, the $\pi/2$-BPSK technique adds very little extra complexity. On the other hand, because the TR-based technique requires FFT/IDFT computations for both the projection and iterative clipping procedures, it has an increased computational cost. As a result, whereas $\pi/2$-BPSK with TR significantly reduces PAPR, it comes with a trade-off with computational complexity.

IV. Conclusion

This study used a unified simulation framework to compare QPSK DFT-s-OFDM, $\pi/2$-BPSK DFT-s-OFDM, and $\pi/2$-BPSK incorporating tone reservation (TR) in 2×2 and 4×4 MIMO systems. The findings demonstrate that $\pi/2$-BPSK offers intrinsic PAPR reduction over QPSK because of better envelope characteristics, whilst the inclusion of TR leads in a total reduction of roughly 2.5–3 dB at a CCDF of 10^{-3}. Both MIMO configurations show the same improvement. While the TR-based system preserves BER performance comparable to $\pi/2$-BPSK DFT-s-OFDM, its principal benefit lies in achieving additional PAPR reduction without introducing distortion to the data-bearing subcarriers. From a complexity perspective, TR adds extra computational cost because of iterative processing, although $\pi/2$-BPSK has no overhead. All

TABLE IV: Computational Complexity Comparison

Scheme	**Relative Complexity**
QPSK DFT-s-OFDM	Baseline (DFT + IDFT)
$\pi/2$-BPSK DFT-s-OFDM	Baseline + Phase Rotation ($O(M)$)
$\pi/2$-BPSK + TR	Baseline + TR Iterations ($O(KN \log N)$)

things considered, $\pi/2$-BPSK with TR is a viable option for power-efficient uplink transmission in MIMO DFT-s-OFDM systems since it provides an efficient trade-off between PAPR reduction and complexity.

REFERENCES

[1] G. Berardinelli, "Generalized dft-s-ofdm waveforms without cyclic prefix," *IEEE Access*, vol. 6, pp. 4677–4689, 2018.

[2] H. Deng, J. Xu, and L. Liu, "Bit error rate analysis for dft-s-ofdm systems under impulsive noise," *IEEE Communications Letters*, vol. 28, no. 5, pp. 1176–1180, 2024.

[3] R. Li, G. Li, P. Zhang, and F. Gong, "Bit error rate performance of dft-s-ofdm systems under alpha-stable noise," *IEEE Communications Letters*, vol. 29, no. 3, pp. 645–649, 2025.

[4] A. N. Aljalai, C. Feng, V. C. Leung, and R. Ward, "Improving the energy efficiency of dft-s-ofdm in uplink massive mimo with barker codes," in *2020 International Conference on Computing, Networking and Communications (ICNC)*, pp. 731–735, 2020.

[5] K. R. Gudimitla, M. S. A. Khan, S. Amuru, and K. Kuchi, "Pre-dft multiplexing of reference signals and data in dft-s-ofdm systems," *IEEE Open Journal of the Communications Society*, vol. 5, pp. 514–525, 2024.

[6] B. Gouda, I. Atzeni, and A. Tlli, "Uplink transmit power optimization for distributed massive mimo systems with 1-bit adcs," *IEEE Transactions on Wireless Communications*, vol. 25, pp. 9094–9110, 2026.

[7] M. Shi, F. Wang, M. Zhang, Z. Wang, and N. Chi, "Papr reduction of 2.0gbit/s dft-s ofdm modulated visible light communication system based on interleaved sub-banding technique," in *2017 IEEE International Conference on Communications Workshops (ICC Workshops)*, pp. 337–342, 2017.

[8] Y. s. Tek, E. B. Tuna, K. Karaerik, H. Sinop, S. Yaar, B. Avc, G. Aykr, and A. zen, "A novel papr improvement approach for the next generation waveforms," in *2020 43rd International Conference on Telecommunications and Signal Processing (TSP)*, pp. 658–662, 2020.

[9] s. S. etiner, B. Dumlu, A. Savachabe, and A. zen, "A novel papr reduction technique combining the pts and clipping method," in *2021 44th International Conference on Telecommunications and Signal Processing (TSP)*, pp. 394–398, 2021.

[10] L. Yang, L. Dan, Y. Hu, P. Yang, and S. Zammit, "On the channel estimation of low-papr waveform for 5g evolution and 6g," in *2023 IEEE 98th Vehicular Technology Conference (VTC2023-Fall)*, pp. 1–5, 2023.

[11] S. Gkceli, I. Peruga, E. Tiirola, K. Pajukoski, T. Riihonen, and M. Valkama, "Novel tone reservation method for dft-s-ofdm," *IEEE Wireless Communications Letters*, vol. 10, no. 10, pp. 2130–2134, 2021.